FR 82 p 1728

IPNO-PhN-81-18

ORSAY AND SATURNE NEW RESULTS ON (p,π) AND (ION,π) EXPERIMENTS

Y. LE BORNEC and N. WILLIS

Institut de Physique Nucléaire, BP N°1
91406 ORSAY, France

Invited talk at
"Workshop on Pion Production and Absorption in Nuclei".
Bloomington, Indiana,
22, 24 Octobre 1981.

institut de physique nucléaire LABORATOIRE ASSOCIÉ A L'IN2P3

UNIVERSITÉ PARIS-SUD

IPNO-PhN-81-18

ORSAY AND SATURNE NEW RESULTS ON (p,π) AND (ION,π) EXPERIMENTS

Y. LE BORNEC and N. WILLIS

Institut de Physique Nucléaire, BP N°1
91406 ORSAY, France

Invited talk at
"Workshop on Pion Production and Absorption in Nuclei".
Bloomington, Indiana,
22, 24 Octobre 1981.

ORSAY AND SATURNE NEW RESULTS ON (p,π) AND (ION,π) EXPERIMENTS

Y. Le Bornec and N. Willis
Institut de Physique Nucléaire, BP n°1
91406 Orsay, France.

ABSTRACT

New results of (p,π) reaction on light target nuclei (^{3}He, ^{4}He, ^{6}Li, ^{10}B) have been obtained at IPN Orsay. Data on (^{3}He,π^+) reaction on the same targets, in the exclusive kinematical region are presented together with data on ^{6}Li(d,π^-)^{8}B reaction obtained at Saturne.

INTRODUCTION

High momentum transfer processes such as coherent (p,π) or (p,d) reactions have been investigated intensively in medium energy nuclear physics over the past decade but there is still much controversy surrounding the basic reaction mechanisms. In order to disentangle the mechanism from the nuclear structure, we have performed (p,π) experiments [1] on light nuclei for which the wave functions are considered well-known. It could be that further valuable clues are also provided by reactions which involve the transfer of several nucleons and for that purpose we have started a program to study coherent pion production with composite projectiles. The hope was therefore to determine to what extent the different nucleons of the projectile and the target are collectively involved in the production of the pion.

In this paper experimental data on (^{3}He,π) [1] and (d,π) [2] reactions near and below the threshold for production in free NN → NNπ reactions will be presented.

I - EXPERIMENTAL PROCEDURE

1° The synchrocyclotron. After a shutdown for change over, the rebuilt Orsay synchrocyclotron has been operating since the end of 1978. Proton, deuteron, ^{3}He and ^{4}He external beams have been delivered. The main characteristics of the machine are presented in the table n°1.

Moreover, for one year, the energy has been continuously variable between the lower and the upper values given in the table. A scheme of the machine and of the experimental areas is presented in figure n°1.

A duty cycle up to 40 % can be obtained when using the slow extraction system. The energy dispersion of the extracted beam is about $\frac{\Delta E}{E} = \pm 3.5 \times 10^{-3}$. However, slits on the analysed beam line (used for the π production experiments) permit one to reduce this value down to $\pm 3 \times 10^{-4}$. An overall resolution of 40 keV has been achieved with 201 MeV protons by means of an energy loss spectrometer located on the other beam line.

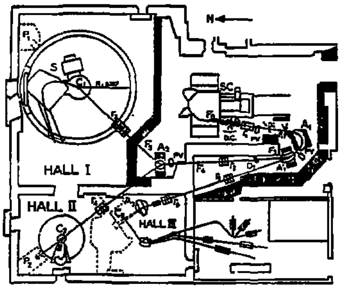

Fig. I. Orsay synchrocyclotron : the machine and the experimental areas.

On line spectroscopic measurements are performed on the third line "Isocele".

2° Experimental set-up for pions production experiments.

The layout is shown in figure 2. The pions were focussed by a quadrupole doublet onto a scintillator A located in the object focal plane of a 180° spectrometer (radius R = 57.5 cm). This makes possible the analysis of particles with a maximum magnetic rigidity of .9Txm with a solid angle $\Delta\Omega = 6.2 \times 10^{-3}$ sr. This last value is for the studied pions instead of 6×10^{-5}Sr for particles of different momenta coming from the target. This factor of 100 is important for counting rates in detector A.

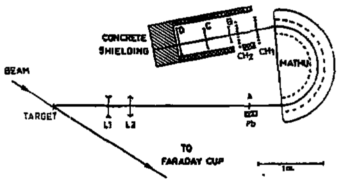

Fig. 2. Experimental set-up.

The momentum acceptance is about ± 2.5 %. The entire apparatus can be rotated around the target axis between 20° and 155°. The whole flight path of the pions is about 6.8 meters, the main part of which is in a continuous vacuum. It has to be remarked that all the elements of the spectrometer were salvaged from other equipment and that this whole apparatus was quite inexpensive.

The incident beam is in vacuum up to the Faraday cup in the beam dump. An additional relative monitoring is furnished by a 3 scintillators telescope which views the target.

The particles trajectories were determined by means of two multiwires chambers with cathode readout providing a spatial resolution of about .3 mm. These chambers which accept high counting rates are triggered by a four fold coincidence A.B.C.D.

Event-by-event calculation of the focal plane position and the trajectory angle relative to the optical axis provided the on-line monitoring of the experiment. Only those particles satisfying conditions on the time of flight between A & B and B & D and vertical position in the chambers were considered. However all events were kept for storage on magnetic tape to allow replay and optimal event selection. Dead times are measured with a pulse generator on each photomultiplier and chamber.

The reactions involving ^{3}He or ^{4}He targets were studied with the help of the Orsay Cryogenic helium target, the walls of which are very thin ($\sim$ 12 μm steel). Target-empty runs determined the background from interactions in the target walls.

II - (p,π) RESULTS

A - TYPICAL SPECTRA

1° $^3He(p,\pi^+)^4He$ and $^4He(p,\pi^+)^5He$. Details on $^3He(p,\pi^+)^4He$ experiment can be found in ref. [3] and we just briefly summarize here some points.

On-line typical spectra (without background subtraction) are shown on figure 3 for $T_p = 201$ MeV, with an average intensity of 130 nA on a 110 mg/cm^2 ^{3}He target and 103 mg/cm^2 ^{4}He target.

The pion energy was typically 42 MeV in the case of $^3He(p,\pi^+)^4He$ reaction and 24 MeV for the $^4He(p,\pi^+)^5He$.

The ^{5}He nucleus is unbound and not well known (position of the first excited state 4 ± 1 MeV and width 4 ± 1 MeV) so that the peak corresponding to the ground state could not be precisely extracted. The dashed line represents a phase space calculation for the 3 body reactions subtraction (6).

2° $^6Li(p,\pi^+)^7Li$ and $^{10}B(p,\pi^+)^{11}B$. These spectra (figure 4)were obtained in measurements of only 30 minutes with a 150 nA beam intensity for the 43.25 mg/cm^2 ^{6}Li target thickness. The energy resolution was about 300 keV. It can be noticed that the $7/2^-$ (4.63 MeV) level is highly excited despite the fact that the one step process is strongly suppressed. This already was observed at 600 MeV in Saclay experiments [4] a few years ago.

It is well known that the high spin levels are generally the most excited states in the (p,π) reactions.

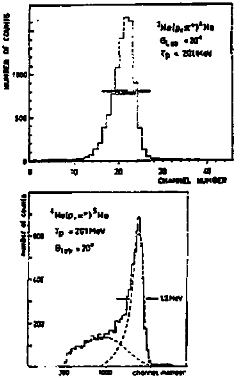

Fig. 3. $^{3}He(p,\pi^{+})^{4}He$ and $^{4}He(p,\pi^{+})^{5}He$ typical spectra at T_p = 201 MeV, θ_{lab} = 20°.

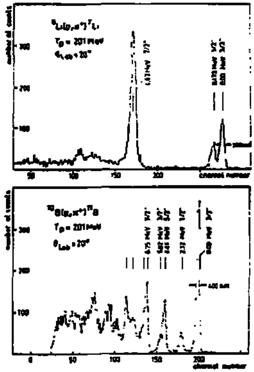

Fig. 4. $^{6}Li(p,\pi^{+})^{7}Li$ and $^{10}B(p,\pi^{+})^{11}B$ typical spectra at T_p = 201 MeV, θ_{lab} = 20°.

B - ANGULAR DISTRIBUTIONS

The angular distributions of the ^{3}He data at several energies are shown in the figure 5 where the error bars take into account statistical effects and uncertainties due to the overlapping of the three different magnetic fields which lead to the same peak. This effect becomes important for the lowest energy pions and hence for the largest angles. The absolute cross sections are obtained with an overall uncertainty of ± 20 %. The main uncertainties are due to the determination of the solid angle, the detection efficiency, the target thickness, and the beam monitoring.

It should be pointed out that the cross sections are high, of the order of magnitude of several μb/sr. The angular distributions are structureless and smooth with θ_{cm} variation. The transferred momentum at forward angles which is not very energy dependent is typically 2 fm^{-1}. The same type of comments can be done for the angular distribution on ^{4}He and the cross sections are of the same order of magnitude. Figure 6 represents the cross section variations versus the incident energy at an angle of 20°. The data from Saturne [5] are also presented. One can see the bump probably due to the influence of the (3,3) resonance and the strong decrease of the

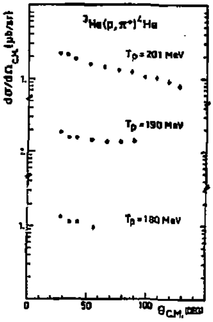

Fig.5.Angular distributions for $^3He(p,\pi^+)^4He$ reaction at different incident energies.

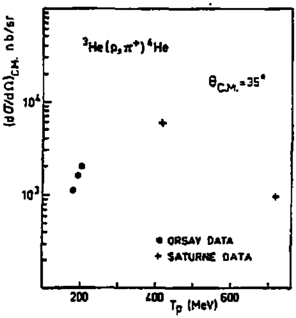

Fig.6. Differential $^3He(p,\pi^+)^4He$ cross-section versus incident energy. Crosses correspond to data from ref.(5) and circles correspond to our data.

cross sections at lower energies, partly due to the decrease of the phase space factor.

The range of pion energies covered allows us to make an extrapolation to zero energy so that a comparison with the results obtained from pionic atoms becomes possible.

In terms of a centre-of-mass amplitude f and momentum k^*, the unpolarised pion production cross section is

$$(d\sigma/d\Omega)^*_{p\,^3He \to \pi\,^4He} = (k^*_\pi/k^*_p)\,\overline{|f^2|} \tag{1}$$

where the bar denotes averaging over the initial proton and ^3He spins. At threshold the only contributions to the imaginary part of the elastic $\pi\alpha \to \pi\alpha$ amplitude, calculated via the optical theorem, comes from the absorption cross section so that

$$k^*_\pi\,\sigma_{\pi\alpha \to abs} = 4\pi\,\mathrm{Im}(f_{\pi\alpha \to \pi\alpha}) \tag{2}$$

where the limit $k^*_\pi \to 0$ is understood. The right hand side may be estimated from the pionic atom shifts and widths [7] which give

$$\mathrm{Im}(f_{\pi\alpha \to \pi\alpha}) = 0.042 \pm 0.003 \text{ fm}$$

The branching ratio in the pionic atom to the particular nt channel is [8] [9] B = (19 ± 1) % and, assuming that the capture takes place from the s orbit, this enables us to calculate the nt production rate

$$k_\pi^* \sigma_{\pi\alpha \to nt} = 4\pi B \mathrm{Im}(f_{\pi\alpha \to \pi\alpha}) \tag{3}$$

Since there is no angular dependence in the threshold cross sections we can then extract the $nt \to \pi\alpha$ scattering amplitude, defined in equation (1), through the use of detailed balance :

$$\overline{|f^2|}_{k_\pi^* = 0} = (B/4\, k_p^*) \mathrm{Im}\, (f_{\pi\alpha \to \pi\alpha})$$

$$= (9.4 \pm 0.7) \times 10^{-4} \text{ fm}^2$$

This value can be compared to the values (included in the table n°2) deduced from our data.

Angular distributions on ^{6}Li et ^{10}B targetsare plotted in the figure n° 7. Results from Indiana are in good [21] agreement with ours on the ^{10}B target.

We have just to mention the strong decrease of cross - sections by about an order of magnitude between ^{3}He, ^{4}He and ^{6}Li.

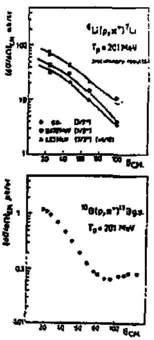

Fig. 7. Angular distributions for ^{6}Li(p,π^+)^{7}Li and ^{10}B(p,π^+)^{11}B reactions at T_p = 201 MeV.

III - (^{3}He,π) AND (D,π) REACTIONS

Although a great deal of experiments (cross section and asymmetry measurements) in proton induced pion production is now available, few results on exclusive production with heavier projectiles have been reported until now. The most recent ones are from LAMPF [10] with (π^+d) studies at T_π = 48 MeV on light nuclei and from CERN by Aslanides et al. [11] with (^{3}He,π^-) measurements done on ^{6}Li at 900 MeV incident energy. This last one shows evidence for exclusive final states with a cross section of about 10 pb/sr. The kinetic energy/nucleon of the projectiles for experiments that we have carried out in Orsay and at Saturne was below the threshold for the production on a free proton. Moreover the transferred momenta are important, so that very low cross sections were expected

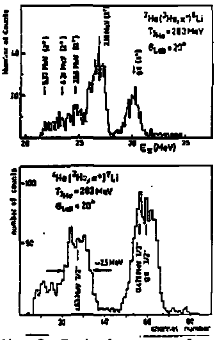

Fig. 8. Typical spectra for ^{3}He(^{3}He,π^+)^{6}Li and ^{4}He(^{3}He,π^+)^{7}Li at $T_{^3He}$ = 283 MeV.

<u>A - (^{3}He,π)</u>. The first set of measurements we will present was performed at the synchrocyclotron in Orsay with ^{3}He projectiles. The incident energy was about 90 MeV/nucleon. The data were taken in the same experiments as the (p,π) data on the same targets.

Typical spectra for ^{3}He(^{3}He,π)^{6}Li and for ^{4}He(^{3}He,π^+)^{7}Li at $T_{^3He}$ = 283 MeV are shown on figure n° 8. For this type of experiment the different energy losses of the ^{3}He and π through the target was the main contribution to the experimental peak which was found to be ∿ 1.5 MeV. In the case of the ^{3}He target, the ground state (1^+), 2.18 MeV (3^+) and 3.56 MeV (0^+) levels are resolved. The relative excitation of the different levels will be discussed later on. The important excitation of the 3^+ level (2.18 MeV) should be noticed. For the ^{4}He(^{3}He,π^+)^{7}Li reaction it can be seen with the preliminary results that the ground state ($3/2^-$) and 0.478 MeV ($1/2^-$) level were not resolved. The 4.63 MeV ($7/2^-$) state is clearly seen. A measurement was also made for pions beyond the kinematical limit and as it can be seen the signal/background ratio is quite good.

Corresponding angular distributions are shown in figure n° 9. The error bars include statistical uncertainties. A systematic uncertainty of ± 20 % was found due to beam calibration, target thickness, solid angle and efficiency determinations.

Several features can be emphasized.

1° The cross sections have about the same order of magnitude (∿ a few tens of nb/sr) on ^3He and ^4He targets. This is quite high yield at such a low energy with transferred momenta of about 3 fm^{-1}. It must be kept in mind for comparison that (p,π) reactions cross sections are about two orders of magnitude higher with transferred momenta of about 2 fm^{-1}.

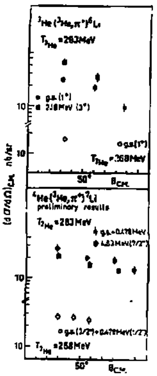

Fig. 9. $^3He(^3He,\pi^+)^6Li$ and $^4He(^3He,\pi^+)^7Li$ angular distributions at different energies.

The low pion energy in $^3He(^3He,\pi^+)^6Li$ reaction allows us to make a comparison with the results obtained from pionic atoms for the ^6Li ground state as we did earlier in the case $^3He(p,\pi^+)^4He$ reaction. With very simple approximations described in ref. [12] agreement with experiment is as good as could be expected i.e. the amplitudes in the centre of mass system are of the same order of magnitude.

2° The ratio R of the cross sections yielding the 2.18 MeV and ground states of ^6Li at the same laboratory angle is about 1.7. In low energy transfer reactions, where the mechanism could be completely different, values of the same order of magnitude are found [13]. In the case of $^4He(^3He,\pi^+)^7Li$ the 7/2$^-$ excited state and the two first levels doublet are equally excited. Any theoretical model has to reproduce these features.

The $(^3He,\pi)$ reaction on ^6Li and ^{10}B targets has also been investigated at 260 MeV, 270 MeV and 283 MeV at θ_{lab} = 20°. A typical spectrum on a ^6Li target is shown in figure 10. The ground state (3/2$^-$) and 2.43 MeV (5/2$^-$) levels are clearly resolved. The peak/background ratio is fairly good. This spectrum was obtained in 16 hours with an average intensity of 350 nA. A very preliminary analysis leads to cross sections of about 100 pb/sr for the ground state of ^9Be which is more than two orders of magnitude lower than cross sections on ^3He and ^4He targets. Nevertheless the transferred momentum is about 3.6 fm^{-1}.

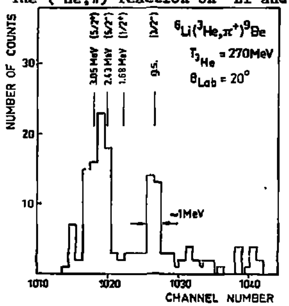

Fig. 10. Typical spectrum for $^6Li(^3He,\pi^+)^9Be$ reaction at $T_{^3He}$ = 283 MeV.

B - (D,π) REACTION

Another experiment using deuteron beam was carried out at the Saturne National Laboratory (LNS) by a collaboration CRN Strasbourg, IPN Orsay and DPhNME/Saclay with the high resolution spectrometer SPES I. (d,π^-) reactions have been studied at 150 MeV/nucleon and 300 MeV/nucleon on ^6Li, ^9Be and ^{10}B targets [14]. The detection of π^- instead of π^+ minimizes the background due to the target through the spectrometer. Due to the very low counting rates, inclusive spectra only are measured on ^9Be and ^{10}B near the kinematical limit. Both exclusive and inclusive spectra were obtained on the ^6Li target.

We briefly describe the experimental set-up which will be covered in greater detail, by P. Couvert [15]. The basic detection system consisted of five planes of scintillation hodoscopes and three lucite Cerenkov counters. The particle trajectories were determined with 4 two fold drift chambers triggered by a coincidence of the plastic counters. In addition the time of flight was measured between the first and fifth plane of scintillation counters. All calibration and efficiencies were checked using the $p + p \rightarrow d + \pi^+$ reactions. The absolute cross sections were obtained with an overall uncertainty of 20 %. The measurements were performed at 15° (lab) which was a compromise to lower the background while keeping the pion rate measurable. The maximum intensity of the deuteron beam was $\sim 10^{11}$ deuterons/burst. ($\sim$ 15 nA). The data for the inclusive reactions are plotted in figure n° 11 in the form of Lorentz invariant cross sections versus the usual variable $x = \frac{k_{/\!/}\ (CM)}{k_{/\!/Max}(CM)}$, for the three targets. The previous data from Papp et al. [16] at 1,05 GeV/nucleon are also partially presented for comparison. One can summarize several features.

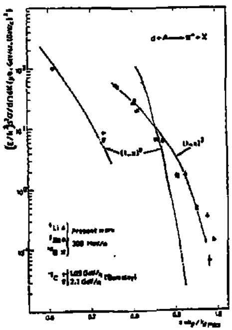

Fig. 11. Inclusive pion spectra induced by 600 MeV deuterons. Results of ref. [16] are also partially presented. The curves are the theoretical binomial shapes $(1-x)^n$.

1° The shape of the spectra is independent of the target as has previously been observed for small x, implying that the projectile structure dominates the pion spectra observed at forward angles.

2° For x = 0.75 the data from Berkeley [16] are lower than ours by about one order of magnitude. This difference cannot be explained even if the transverse momentum $k_\perp$ due to non zero experimental angles is removed. Hence the scaling behaviour which was one of the most striking feature at energies above

1 GeV/nucleon does not persist down to 300 MeV/Nucleon.

3° In the frame of recent theoretical models [17], the invariant cross sections can be parametrized as $(1-x)^n$ where the exponent n is related to the number of constituents and to the basic interactions of the model. For (d,π^-) experiment [16] at high energy, the value n = 9 is clearly favoured as can be seen in figure n° 11, in agreement with the theory [17]. Our data can be fitted by a function $(1-x)^n$ with n = 3. This exponent behaviour is not explained near $x \sim 1$ for such low incident energy.

Typical spectra for the two body reaction $^6Li(d,\pi^-)^8B$ are shown in figure n° 12 at 600 MeV and 300 MeV incident energies. The ground and first excited states are not well separated at 600 MeV due to the target thickness, but the second excited state is clearly seen. The spectrum at 300 MeV was obtained with a thinner target and the experimental resolution of 0.3 MeV (FWHM) permits a clear separation of the three levels.

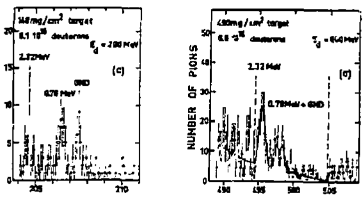

Fig. 12. Pion spectra of the reaction $^6Li(d,\pi^-)^8B$ at 15° (lab.) at 600 MeV and 300 MeV incident energy.

Differential cross sections are presented in table 3. They are found to be very low, and the most striking feature is that they are higher by about a factor of 5 to 8 at the lower energy of 150 MeV/nucleon, suggesting a strong influence of the transferred momentum ($q = 4.6\ fm^{-1}$ and $5.8\ fm^{-1}$ at 300 MeV and 600 MeV respectively) eventhough the energy per nucleon is far below the $NN \rightarrow NN\pi$ threshold.

C - SOME TRENDS OF THE (ION,π) REACTIONS

Despite the scarcity of the data, summarized in figures N° 13 and N° 14, we can try to see some trends in the (ion,π) reactions.

1° The cross sections obtained with an ^3He projectile at $T_{^3He}$ = 283 MeV are about the same for ^3He and ^4He targets, then decrease drastically (almost three orders of magnitude) when changing the target mass number from A = 4 to A = 6. Although much less pronounced, this decrease with A seems to be confirmed by a very preliminary result we have obtained with a ^{10}B target. Indeed this is just a rough comparison because of the difference between the transferred momenta involved in the different reactions.

2° For each composite projectile and a given target (^{6}Li) the cross sections first increase near threshold then strongly decrease when the incident energy goes up. It is clear that a maximum occurs at an incident energy higher than 283 MeV with an ^{3}He projectile. It is difficult to conclude definitively for (d,π) reaction because the data at 100 MeV/nucleon was obtained on a different target nucleus (reverse reaction $^{12}C(\pi^+,d)^{10}C$ at LAMPF [10]), however the same behaviour seems to occur. This effect has not been observed for (p,π) reaction on ^{6}Li considering results from Orsay (201 MeV) LAMPF [18] (equivalent energies T_p = 245 and 360 MeV) and Saturne (T_p = 600 MeV) [4].

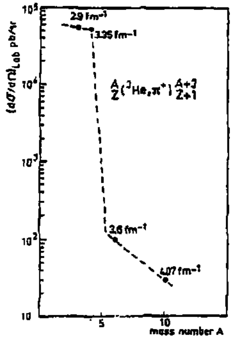

Fig. 13. Variation of the cross-sections for (^{3}He,π^+) on various targets versus the mass number A at 283 MeV incident energy.

3° The ratio of the pion production cross sections for p,d,^{3}He incident projectiles on the same target are approximately 1 : 10^{-3}:2.5 x10^{-5} respectively.

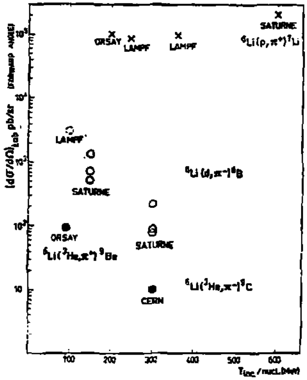

Fig. 14. Variation of the cross sections for the reaction A(a,π)B versus the incident energy/nucleon for different projectiles on ^{6}Li target.

IV - CONCLUSION AND PLANS FOR THE FUTURE

The (ion,π) reactions present very typical characteristics implying strong constraints for theoretical calculations. The present data has been useful as a starting point for theoretical works which will be presented at this workshop by their authors [19] [20].

Further studies of this type of reactions will be carried out at different energies near threshold on ^{6}Li and heavier targets. This is possible considering that high intensity ^{3}He beam is available in Orsay and that pions are clearly identified. Pion production with α particles will also be investigated.

Moreover these measurements should be extended at higher energies with Saturne II facilities.

Table I : Main characteristics of the Orsay synchrocyclotron external beams.

Particles	Energy (MeV)	Maximum extracted intensity (used for on line spectroscopy)
p	167 → 201	2-3 μA
d	91 → 108	
^{3}He	238 → 283	
α	182 → 218	

Table II : Coulomb corrected average squared matrix element extracted from the present data. The overall normalization uncertainty of 20 % has not been included in the error bars.

T_p (MeV)	k^*_π(MeV/c)	$\overline{\lvert f^2 \rvert}$ (10^{-4} fm^2)
180	59	10.9 ± 0.2
190	75	11.9 ± 0.2
201	90	11.9 ± 0.2

Table III : Values of ^{6}Li(d,π$^-$) differential cross section measured at 300 MeV and 600 MeV incident energy, leading to the ground state (2^+), and the two first excited states (0.78 MeV), (2.32, 3^+) of ^{8}B.

	Incident energy E_d	
Levels	300 MeV	600 MeV
0	521 ± 120 pb/sr	75 ± 27 pb/sr
0.78 MeV	707 ± 142 pb/sr	84 ± 27 pb/sr
2.32 MeV	1333 ± 163 pb/sr	237 ± 38 pb/sr

REFERENCES

1. This work in Orsay has been done by : L. Bimbot, M.P. Combes, J.C. Jourdain, N. Koori, Y. Le Bornec, F. Reide, A. Willis and N. Willis.
2. This work at Saturne national Laboratory has been done by E. Aslanides, A.M. Bergdolt, O. Bing, P. Fassnacht, F. Hibou (CRN Strasbourg), N. Willis, P. Kitching, Y. Le Bornec, B. Tatischeff (IPN Orsay), K. Baba, A. Boudard, G. Bruge, P. Couvert and B. Nefkens (DPhN/ME Saclay).
3. N. Willis et al., Journal of Physics G 7 (1981) 195.
4. T. Bauer et al. Phys. Lett. 69B (1977) 433.
5. B. Tatischeff et al. Phys. Lett. 63B (1976) 158.
6. K. Gabathuler et al. Nucl. Phys. B40 (1972) 32.
7. J. Hüfner et al., Nucl. Phys. A231 (1974) 455.
8. M. Bloch et al., Rev. Lett. 11 (1963) 301.
9. R. Bizzarri et al., Nuovo Cimento 33 (1964) 1497.
10. J.F. Amann et al., Phys. Rev. Lett. 40 (1978) 758.
11. E. Aslanides et al., Phys. Rev. Lett. 43 (1979) 1466; 45 (1980) 1738.
12. Y. Le Bornec et al., to be published.
13. J.S. Vincent and E. Boschitz, Nucl. Phys. A143 (1970) 121.
14. E. Aslanides et al., to be published in Phys. Lett.
15. P. Couvert, contribution to this workshop.
16. J. Papp et al., Phys. Rev. Lett. 34 (1975) 601.
17. I.A. Schmidt and R. Blankenbecler, Phys. Rev. D15 (1977) 3321.
18. J. Källne et al., Phys. Rev. C21 (1980) 2681.
19. J.F. Germond, contribution to this workshop.
    J.F. Germond and C. Wilkin, to be published in Phys. Lett.
20. M.G. Hüber, contribution to this workshop.
    M.G. Hüber, M. Dillig and K. Klingenbeck, contribution to 9^{th} ICOHEPANS, Versailles (1981) 202.
21. F. Soga et al., Phys. Rev. C 22 (1980) 1348.